



# Optics Letters

## Spectrally efficient multi-service fiber-wireless access in low-cost direct-detection THz system at 300 GHz

YUANCHENG CAI,<sup>1,2</sup>  SHITONG XIANG,<sup>2</sup> MIN ZHU,<sup>1,2,\*</sup>  WEI LUO,<sup>2</sup> MINGZHENG LEI,<sup>1</sup>  JIAO ZHANG,<sup>1,2</sup>  BINGCHANG HUA,<sup>1</sup> YUCONG ZOU,<sup>1</sup> MIAOMIAO FANG,<sup>2</sup> LIANG TIAN,<sup>1</sup> XINGYU CHEN,<sup>1</sup> AND JIANJUN YU<sup>1,3</sup>

<sup>1</sup>Purple Mountain Laboratories, Nanjing 211111, China

<sup>2</sup>National Mobile Communications Research Laboratory, Southeast University, Nanjing 210096, China

<sup>3</sup>Fudan University, Shanghai, 220 Handan Road, 200433, China

\*minzhu@seu.edu.cn

Received 26 June 2023; revised 3 August 2023; accepted 5 August 2023; posted 7 August 2023; published 22 August 2023

**This Letter demonstrates a novel, to the best of knowledge, overlapping single-sideband (OSSB) transmission scheme for spectrally efficient multi-service fiber-wireless (FiWi) access in a low-cost direct-detection (DD) THz system. Utilizing the proposed OSSB scheme, user data from different services can share the same spectrum resource yet can be successfully demodulated via one cost-effective DD THz receiver in conjunction with the Kramers–Kronig (KK) based SSB field reconstruction and look-up table (LUT) enabled signal separation algorithms. A proof-of-principle experiment is conducted. Based on an IQ modulator and a single THz zero-bias diode (ZBD), two independent 10-Gb/s quadrature phase shift keying (QPSK) signals with an overlapped spectrum are successfully demodulated after 20-km fiber and up to 3-m wireless transmission at the 300-GHz band. To the best of our knowledge, this is the first demonstration of multi-service FiWi access with an OSSB format in a 300-GHz DD THz system.** © 2023 Optica Publishing Group

<https://doi.org/10.1364/OL.498886>

With the increasing demand for mobile data traffic and the diversity of business, it is crucial to support multi-user and multi-service access simultaneously in upcoming 6G networks [1]. In this context, the terahertz (THz) band has attracted much attention for large-capacity wireless fronthaul/backhaul applications, due to its inherent huge bandwidth up to nearly 10 THz [2]. Figure 1 shows a typical THz wireless backhaul concept diagram, which can well support multi-user multi-service collaborative fiber-wireless (FiWi) access. This has been proven to be a very effective solution, especially in some scenarios where fiber is not available [3].

In recent years, many works have been devoted to improving the resource utilization of multi-signal transmission [4] in fiber and/or wireless access system, to reduce its overall cost and increase the spectral efficiency (SE) while providing multi-user and multi-service access capability. A brief summary is given in Table 1. Taking dual signal transmission

as an example, the overlapping double-sideband (ODSB) is a simple but effective scheme. Leveraging on this, two independent DSB signals sharing the same spectrum resource can be simultaneously transmitted and demodulated. Based on IQ modulation and coherent detection, two 1-Gbps independent overlapping quadrature phase shift keying (QPSK) DSB signals are transmitted over 25-km fiber for the first time [5]. Employing cascade amplitude and phase modulation, Chen and Yao also demonstrate the ODSB transmission of a 1.25-Gbps QPSK and a 2.5-Gbps 16-QAM signals over 25-km fiber [6]. However, in addition to relying on an expensive optical coherent receiver, polarization division multiplexing (PDM) is also adopted but does not double the SE as expected in the above two works.

The twin single-sideband (SSB) modulation technique, which utilizes the left and right sidebands to carry different service information, can also achieve the simultaneous transmission of dual signals. Employing the SSB format, it can not only achieve the same SE as the ODSB scheme, but also overcome the problem of the chromatic dispersion-induced power fading effect encountered by traditional DSB or ODSB signals after fiber transmission [11]. The feasibility of two or four signals for FiWi access using a twin-SSB scheme has been successfully demonstrated in single polarization at W band (82 GHz) [7] and dual polarization at Ka band (28.1 GHz) [8], respectively. However, the received twin-SSB signals should be first detected via an electrical heterodyne coherent receiver, which undoubtedly leads to high power consumption. Moreover, the further demodulation of the left or right sideband needs to be separately filtered in the analog or digital domain, which also increases the operation complexity. To solve this problem, a simplified twin-SSB scheme without sideband filtering has been proposed recently [9,10,12]. Through the constellation design for the left and right sidebands in advance, they can be separated using a simple digital de-mapping algorithm instead of traditional complicated sideband filtering. This makes it possible to detect the twin-SSB signals directly via one cost-effective single-end photodiode. The feasibility has been verified in the fiber [9] and

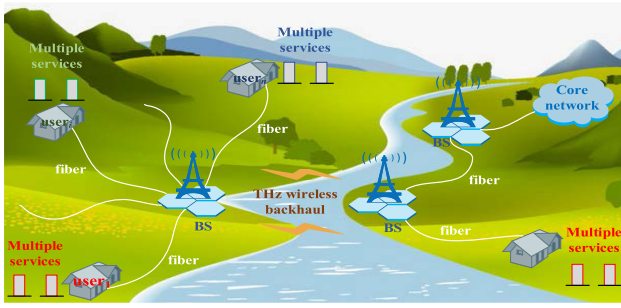


Fig. 1. Concept diagram of multi-user and multi-service access based on the THz wireless backhaul link.

Table 1. Summary of Reported Multi-Signal Transmission Schemes for Multi-Service Fiber and/or Wireless Access

Year	System	Receiver	Scheme	Can PDM Double SE?
2014 [5]	Fiber	Coherent	ODSB	No
2015 [6]	Fiber	Coherent	ODSB	No
2018 [7]	FiWi <sup>a</sup>	Coherent	Twin-SSB	Yes
2021 [8]	FiWi <sup>b</sup>	Coherent	Twin-SSB	Yes
2022 [9]	Fiber <sup>c</sup>	DD	Twin-SSB	Yes
2022 [10]	FSO <sup>c</sup>	DD	Twin-SSB	Yes
This work	FiWi <sup>d</sup>	DD	OSSB	Yes

<sup>a</sup>82 GHz

<sup>b</sup>28.1 GHz;

<sup>c</sup>Verification just by simulation.

<sup>d</sup>300 GHz

four independent SSB vector signals, while occupying the spectrum of only one SSB. Subsequently,  $N$  wavelengths carrying multi-service information are recombined using a wavelength multiplexer (MUX). After optical amplification by an erbium-doped fiber amplifier (EDFA) and transmission over a standard single-mode fiber (SSMF), the combined wavelength division multiplexing (WDM) PDM-OSSB signals are de-multiplexed by another De-MUX. Then for each wavelength, the polarization diversity optical heterodyne detection produces the desired THz OSSB signal in parallel at both  $X$  and  $Y$  polarizations. Next, the above two THz OSSB signals are transmitted over a  $2 \times 2$  multi-input multi-output (MIMO) wireless link. At the receiver, the received two THz OSSB signals are separately downconverted via low-cost THz DD, and then are processed offline to further demodulate the four independent SSB signals in a digital signal processor (DSP). The detailed generation and separation principle of the OSSB signal will be given later.

Based on the simple DD THz receivers,  $4N$  SSB vector signals can be transmitted and demodulated in a WDM system with  $N$  wavelengths. No extra sideband filters are required. This means that the proposed solution can enable multi-user and multi-service access with an appreciable SE due to excellent resource utilization, and meanwhile offers low cost and low power consumption in contrast to expensive heterodyne coherent receivers [2]. The feasibility of the proposed OSSB scheme is verified via a DD THz communication system at 300 GHz by experiment. It clearly outperforms the reported ODSB or twin-SSB scheme by improving the system's SE by nearly double and halving the required bandwidth of digital/analog converters.

The key to achieving the spectrally efficient transmission of multiple signals is the use of the overlapping frequency multiplexing technique, which allows overlapping signal transmission and demodulation based on a DD receiver [13]. One alternative is to control the amplitude and phase of two low-order modulation format signals, then a higher-order modulation format signal can be obtained after superposition [12]. Here we take QPSK as an example. Assume that  $s_1[n]$  and  $s_2[n]$  represent the  $n$ th symbols of two independent QPSK baseband signals with different initial phases of  $0^\circ$  and  $45^\circ$  and whose constellation diagrams are shown in Fig. 3(a) and 3(b), respectively. Since  $s_1[n] \in \{1, i, -1, -i\}$ , when these four types of symbols are separately superimposed with  $s_2[n]$ , it is equivalent to shifting the overall second QPSK constellations by one unit in four different directions: right, up, left, and down, respectively. As a result, the obtained superimposed signal by  $s_1[n] \pm s_2[n]$  has total 16 constellation points, which exactly exhibits the constellation of star-16QAM, as shown in Fig. 3(c). It should be emphasized that the tags  $a_i$ ,  $b_j$ , and  $c_{ij}$  ( $i, j = 1, 2, 3, 4$ ) reveal the unique mapping relationship between the two original QPSK symbols and the superimposed symbols. For instance, the symbol  $c_{12}$  is the superposition of symbol  $a_1$  and symbol  $b_2$ . In this context, a look-up table (LUT) may be established in advance at the receiver side according to the above tags, that is  $c_{ij} \Rightarrow [a_i, b_j]$ . Once the superimposed symbol  $c_{ij}$  is successfully recovered, these two independent QPSK symbols  $a_i$  and  $b_j$  can be effectively obtained through the LUT process.

Considering the simplified verification as well as the limitation of the available equipment, a proof-of-principle experiment for dual QPSK signal transmission on a single polarization over a 300-GHz DD THz link has been conducted. The experimental setup is shown in Fig. 4. In the transmitting DSP of the OSSB optical transmitter, as shown in Fig. 4(a), two different

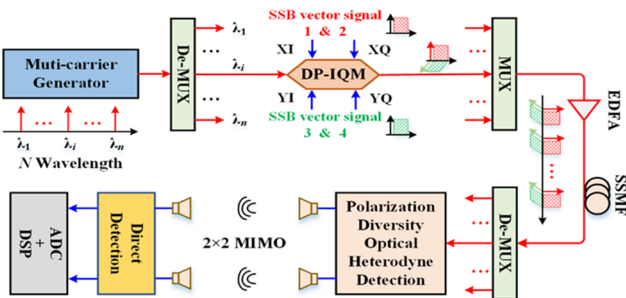
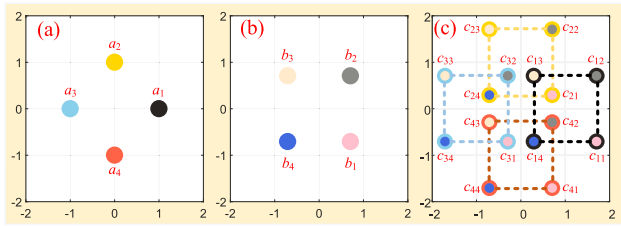


Fig. 2. Concept diagram illustrating multi-service transmission based on OSSB modulation and DD reception.

free-space optical (FSO) [10] communication scenarios only by simulation.

In this Letter, we propose a novel multi-service FiWi access solution employing a spectrally efficient overlapping SSB (OSSB) scheme, which is quite suitable for low-cost direct-detection (DD) THz systems. The concept diagram of our proposed scheme is illustrated in Fig. 2.  $N$  wavelengths originating from one multi-carrier generator are first split by an optical wavelength de-multiplexer (De-MUX). Then for each wavelength, one dual-polarization IQ modulator (DP-IQM) is used to convert two OSSB vector signals from the electrical to the optical domain, so generating one PDM-OSSB signal. What should be emphasized is that each OSSB consists of two independent SSB vector signals with an overlapped spectrum. As a result, the generated PDM-OSSB signal contains



**Fig. 3.** Constellation of QPSK signal with initial phases of (a)  $0^\circ$  and (b)  $45^\circ$ ; (c) constellation of the obtained superimposed signal.

sets of pseudo-random binary sequences (PRBSs) consisting of  $2^{19}$  bits are first mapped into QPSK symbols with distinct initial phases of  $0^\circ$  and  $45^\circ$ , respectively. We use  $s_1(t)$  and  $s_2(t)$  to denote the two independent QPSK signals after upsampling and root-raised-cosine (RRC) filtering. Then an OSSB signal with a virtual carrier can be acquired through the superposition operation of  $s(t) = s_1(t) + s_2(t) + V_C$ , as shown in Fig. 4(b). The term  $V_C = \exp[-j2\pi f_s t]$  represents the virtual carrier which is added to the edge of the OSSB signal. The carrier-to-signal power ratio (CSPR) and guard band (GB) of the OSSB signal can be flexibly adjusted by changing the values of  $V_C$  and  $f_s$ , respectively. It is worth noting that the two independent SSB signals are entirely overlapped in the frequency domain. This means that the dual QPSK signals carrying two different service data can be transmitted simultaneously in a spectrally efficient way, as mentioned above. Subsequently, two 92-GSa/s digital-to-analog converters (DACs) are used to convert the real and imaginary parts of the resampled OSSB signal into analog signals. The required bandwidth of each DAC is only  $f_s/2$ , which is much less than that of the ODSB or twin-SSB schemes when adopting a small or even zero GB. After being amplified by two electrical amplifiers (EAs), the obtained real and imaginary parts are input into an IQM to realize electro-optic modulation. By setting the bias of the IQM to the transmission null point, an optical OSSB signal with carrier can be obtained utilizing the linear conversion from the electrical domain to the optical field. A free-running tunable external cavity laser (ECL), ECL1, with a central wavelength of 1549.316 nm, linewidth of less than 100 kHz, and power of 14 dBm is used as the input laser. After that, the modulated optical OSSB signal is transmitted over a 20-km SSMF. EDFA1 and EDFA2 are used to vary the optical power prior to the SSMF and optical-THz converter, respectively.

At the optical-THz converter, a tunable optical filter (TOF) is used to suppress the out-of-band amplified spontaneous emission noise induced by the EDFAs and Gaussian white noise resulting from the fiber channel. Subsequently, an optical coupler (OC) is used to couple the received signal light with an optical local oscillator (i.e., ECL2), which has a frequency offset of about 300 GHz relative to ECL1. Figure 4(c) shows the combined optical spectra, among them OSSB signals with three different baud rates (2, 6, 10 GBd) are presented. After being amplified by EDFA3, the coupled optical signals are then fed into an ultra-fast uni-traveling carrier photodiode (UTC-PD, IOD-PMJ-13001) to perform optical heterodyne detection. Each UTC-PD has a typical responsivity of 0.22 A/W and an operating wavelength ranging from 1540 nm to 1560 nm. As a result, a 300-GHz THz OSSB signal can be generated, which also includes two independent QPSK SSB signals with an overlapped spectrum, similar to the optical domain. To achieve an optimal optical heterodyne beating effect, two polarization controllers (PCs) are employed to adjust the alignment of the polarization state between the signal and local oscillator lights. Next, a pair of horn antennas (HAs) providing a total gain of  $2 \times 25$  dBi, are employed to transmit the above THz OSSB signal wirelessly within a distance of 3 m.

At the THz wireless receiver, one single low-cost and power-efficient zero-bias diode (ZBD) is used to downconvert the THz OSSB signal to an intermediate frequency (IF), as shown in Fig. 4(d). The ZBD operates from 220~330 GHz with a typical responsivity of 1700 V/W. Afterwards, the IF signal is amplified by two cascaded EAs with a total gain of 33 dB. The signal is then sampled by a 128-GSa/s digital storage oscilloscope (DSO) for subsequent offline digital signal processing. Figure 4(e) shows the workflow of the receiving DSP. After resampling, the Kramers–Kronig (KK) algorithm is adopted to alleviate the signal-to-signal beating interference (SSBI) while reconstructing the transmitted OSSB vector signal. Subsequently, a superimposed baseband signal with star-16QAM constellations can be obtained through baseband recovery, RRC filtering, and least mean square (LMS) equalization. Then, according to the one-to-one mapping relationship via the LUT, it is easy to separate the two independent QPSK symbols from the mixed star-16QAM symbols. Finally, we can calculate the corresponding bit error ratio (BER) of each QPSK signal after symbol de-mapping.

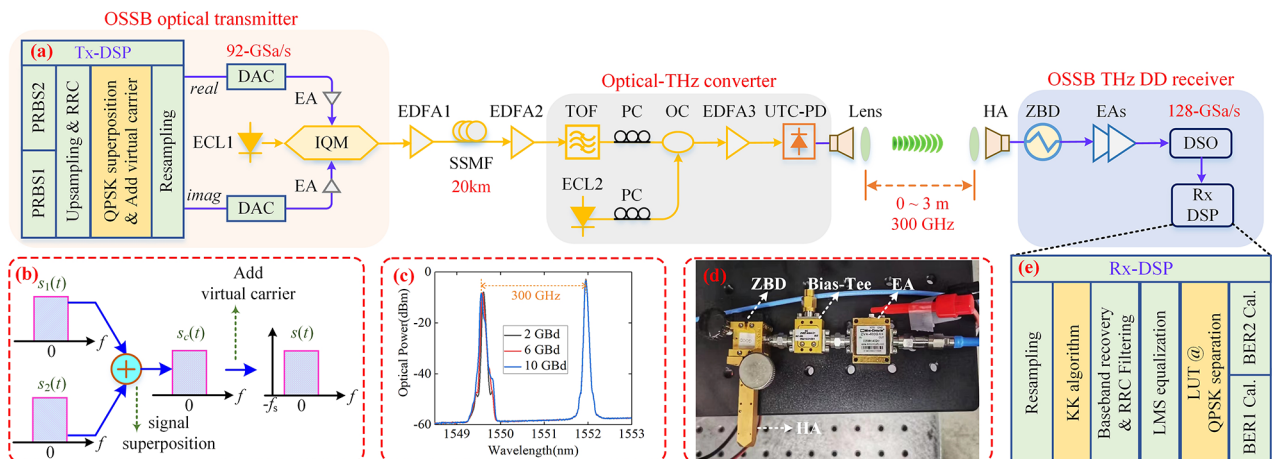


**Fig. 4.** Experimental setup of dual signal transmission employing an OSSB scheme over a 300-GHz DD THz link. (a) Transmitting DSP; (b) generation of OSSB signal; (c) signal optical spectra; (d) photo of low-cost ZBD-based DD THz receiver; (e) receiving DSP.

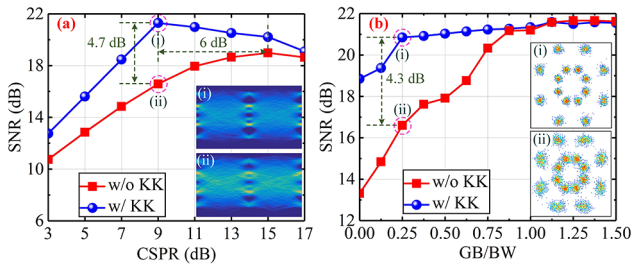


**Fig. 5.** Impact of the KK algorithm on the proposed OSSB transmission scheme under different (a) CSPRs and (b) GBs at the BtB case.

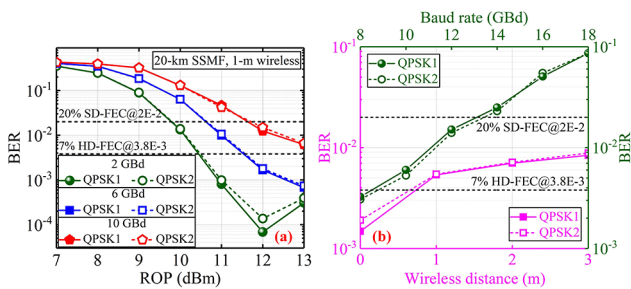


**Fig. 6.** (a) Receiving sensitivity and (b) BER versus the wireless distance or baud rate curves for OSSB-based dual signal transmission.

We first study the impact of KK algorithm on the proposed OSSB transmission scheme under different CSPR values at the optical and THz back-to-back (BtB) case with a baud rate of 2 GBd. The results are shown in Fig. 5(a). Compared to the absence of the KK algorithm, using the KK algorithm not only can reduce the optimal CSPR by 6 dB, but also improve the signal-to-noise ratio (SNR) of the recovered star-16QAM signal by about 4.7 dB under the optimal CSPR of 9 dB. These are mainly attributed to the effective SSBI mitigation. Fixing the CSPR at 9 dB, Fig. 5(b) further presents the impact of the KK algorithm under different GB values. When without the KK algorithm, the SNR improves as the GB increases due to reducing the impact of SSBI and becomes stable until using a full protection interval (i.e., the GB equals the signal bandwidth). Instead, after using the KK algorithm, the SNR can basically stabilize even with a small GB of 0.25 times the bandwidth, benefitting from the considerable mitigation of SSBI. This GB is also selected for the subsequent verification, considering the trade-off between the performance and SE.

Subsequently, employing the proposed OSSB scheme, we investigate the receiving sensitivity for dual signal transmission in a 300-GHz DD THz system. The BER versus received optical power (ROP) of UTC-PD curves under 2-, 6-, and 10-GBd baud rates after 20-km SSMF and 1-m wireless transmission are shown in Fig. 6(a). Firstly, the demodulated two independent QPSK signals, which are recovered from a star-16QAM signal with an OSSB spectrum, have similar BER performances. Secondly, since the signal distortion during amplification and sampling is related to the corresponding signal amplitude, the optimal ROP increases from 12 dBm (2-GBd case) to over 13 dBm (6- and 10-GBd cases) with the increase of baud rate.

Thirdly, at the 7% overhead hard-decision forward error correction (HD-FEC) BER threshold ( $3.8E-3$ ), the required ROP for the 2-GBd and 6-GBd cases are 10.5 dBm and 11.5 dBm, respectively. In contrast, as for the 10-GBd OSSB case, the required ROP to reach the thresholds of 20% soft-decision FEC (SD-FEC) ( $2E-2$ ) and 7% HD-FEC are about 11.7 dBm and above 13 dBm, respectively. We used a maximum input power of 13 dBm in our experiment to protect the UTC-PD from being damaged.

Next, fixing the ROP at 13 dBm, the BER performance is further evaluated under different wireless distances and transmission baud rates. As shown in Fig. 6(b), all the BERs demodulated from the two independent 10-GBd QPSK signals after 20-km fiber and 0~3-m wireless transmission, are lower than the 20% SD-FEC threshold. In addition, under the same 20% SD-FEC BER threshold, the maximum supported baud rate for overlapping QPSK signals is around 13 GBd for 20-km SSMF and 1-m wireless transmission. The total transmission rate of this 300-GHz DD THz link is 52 Gbps.

In conclusion, we propose and experimentally demonstrate an OSSB scheme to achieve spectrally efficient dual signal transmission in a low-cost DD THz link. Two 10-GBd independent QPSK signals with an overlapped spectrum can be simultaneously transmitted over 20-km SSMF and up to 3-m wireless at the 300-GHz band, and successfully demodulated via a simple THz ZBD receiver. The proposed OSSB scheme, in conjunction with mature PDM and WDM techniques, may present a viable strategy to enable high SE and cost-effectiveness for multi-user and multi-service FiWi access in the upcoming 6G networks.

**Funding.** National Natural Science Foundation of China (62101126, 62101121, 62271135); Natural Science Foundation of Jiangsu Province (BK20221194, BK20220210).

**Disclosures.** The authors declare no conflicts of interest.

**Data availability.** Data underlying the results presented in this Letter are not publicly available at this time but may be obtained from the authors upon reasonable request.

**REFERENCES**

1. X. You, C.-X. Wang, and J. Huang, *et al.*, *Sci. China Inf. Sci.* **64**, 110301 (2021).
2. T. Nagatsuma, S. Horiguchi, Y. Minamikata, Y. Yoshimizu, S. Hisatake, S. Kuwano, N. Yoshimoto, J. Terada, and H. Takahashi, *Opt. Express* **21**, 23736 (2013).
3. T. Nagatsuma, G. Ducournau, and C. C. Renaud, *Nat. Photonics* **10**, 371 (2016).
4. P. Li, Z. Dai, L. Yan, and J. Yao, *Opt. Express* **30**, 6690 (2022).
5. Y. Chen, T. Shao, A. Wen, and J. Yao, *Opt. Lett.* **39**, 1509 (2014).
6. X. Chen and J. Yao, *J. Lightwave Technol.* **33**, 1 (2015).
7. R. Deng, J. Yu, J. He, M. Chen, Y. Wei, L. Zhao, Q. Zhang, and X. Xin, *J. Lightwave Technol.* **36**, 5562 (2018).
8. W. Wang, D. Zou, X. Feng, Q. Sui, R. Lu, Z. Cao, and F. Li, *Opt. Express* **29**, 37453 (2021).
9. Y. Zhou, J. Xiao, C. Zhao, J. Zuo, J. Ming, and L. Zhao, *Opt. Express* **30**, 619 (2022).
10. L. Zhao, H. Guo, Y. Liu, J. Xiao, T. Wu, S. Song, and L. Guo, *Opt. Express* **30**, 22946 (2022).
11. J. Yu, Z. Jia, L. Yi, Y. Su, G. Chang, and T. Wang, *IEEE Photonics Technol. Lett.* **18**, 265 (2006).
12. Y. Zhou, J. Ming, L. Wang, D. Wu, L. Zhao, and J. Xiao, *Opt. Lett.* **47**, 5317 (2022).
13. S. Xiang, Y. Cai, W. Luo, J. Zhang, M. Lei, B. Hua, J. Li, and M. Zhu, in *Optoelectronics and Communications Conference (OECC) (IEEE, 2023)*, pp. 1–3.